



# Simulation Research on the Stability of High-Precision Ship-Borne Printer

Zanfu Yang\*, Hao Zheng, Xiaoyong Bai, Xiaolong Jiang

CSSC Marine Technology Co., Ltd., Beijing, China

\*Corresponding author's e-mail: yangzanfu@126.com

**Abstract.** Aiming at the vibration problem of the high-precision ship-borne printer in extreme environments, this paper conducts a systematic study of the dynamic characteristics. First, the finite element method is used to analyze the first six modes of the printer, revealing its natural frequencies and mode shape characteristics. Second, based on the power spectral density data of sea surface vibration velocity under the condition of a Category 12 typhoon, the external excitation response of the printer in extreme environments is simulated. The research results indicate that the vibration response of the high-precision ship-borne printer in the Y-axis direction is the most significant, with a maximum displacement of 0.14446 mm. The first-order modal frequency of the printer is 61.337 Hz, mainly manifested as the local vibration at the supporting interface of the printhead module. A significant resonance response is observed around 60 Hz, but the maximum displacement remains within 20  $\mu\text{m}$ , demonstrating the printer's excellent vibration resistance. Therefore, the results of this study provide important references for structural optimization and vibration reduction design of high-precision ship-borne printers.

**Keywords:** High-Precision Ship-Borne Printer; Vibration analysis; Modal analysis

## 1 Introduction

With the rapid development of marine engineering technology, the high-precision ship-borne printer, as a core component of modern ship navigation systems, plays an irreplaceable role in outputting high-resolution nautical charts and ensuring navigation safety [1-2]. The printing resolution of the printer is a key parameter determining the precision of nautical charts, which directly affects the navigation accuracy and navigation safety of ships. However, during navigation, ships are inevitably subjected to multi-source external excitations, including wave loads, wind load excitations, and engine vibrations, resulting in complex vibration responses of the hull [3-4]. These vibrations are transmitted to the ship-borne printer through the hull structure, potentially affecting its operational stability and printing precision, and may even lead to device failure in severe cases. Therefore, an in-depth study of the vibration characteristics of the high-precision ship-borne printer is essential for optimizing the structural design,

enhancing vibration resistance, and ensuring stable operation in extreme environments. In this paper, a systematic dynamic analysis method is adopted to investigate the problem from two dimensions: intrinsic characteristics and external excitation responses [5-6]. Firstly, the intrinsic characteristics such as natural frequencies and mode shapes of the printer are revealed through modal analysis, and the potential impact of its dynamic characteristics on the performance is evaluated. Secondly, combined with the external excitation conditions under typical sea conditions, vibration response analysis is conducted to comprehensively evaluate the printer's dynamic behavior in actual operating environments [7-8]. The research results provide theoretical basis and technical support for the structural optimization, vibration reduction design, and performance enhancement of high-precision ship-borne printers, and also provide important references for the research of vibration control strategies for high-precision devices operating in extreme environments.

## 2 Methods and Models

The three-dimensional structural model of the high-precision ship-borne printer is shown in Figure 1(a), with overall dimensions of 1437 mm × 482 mm × 559.4 mm. Structurally and functionally, the printer can be divided into four core components: 1. Base plate module: As the connection interface between the printer and the hull, the base plate enhances the stability of the structural connection by expanding the contact area and effectively disperses the vibration excitation from the hull. This module serves as an important force transmission path between the printer and the hull, and its design directly affects the vibration transmission characteristics. 2. Shock-absorbing column assembly: Located between the base plate and the main body of the printer, this component is made of high-damping materials and features an optimized structural design, possessing excellent vibration reduction, deformation resistance, and impact resistance. This assembly can significantly attenuate the vibration energy transmitted from the hull, ensuring a stable operating environment for the precision components inside the printer. 3. Casing structure: Serving as the main frame of the printer, the casing not only provides mechanical support for internal high-precision components but also integrates key functions such as power management, interface communication, print output, and protection of core components. 4. High-precision printhead module: As the core functional component of the printer, the dynamic characteristics and stability of the printhead directly determine the printer's output resolution and printing quality. Its schematic diagram is shown in Figure 1(b).

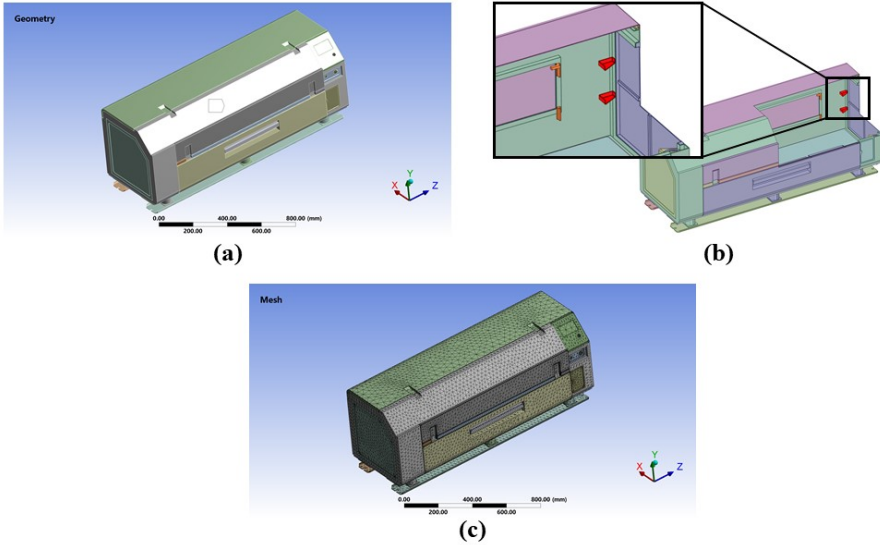


**Fig. 1.** (a) Three-dimensional model of the high-precision ship-borne printer, (b) high-precision printhead module, (c) finite element mesh model diagram of the large display terminal.

The study on the vibration characteristics of the high-precision ship-borne printer consists of two main parts: eigenmode analysis and external excitation response analysis. In terms of eigenmode analysis, the finite element method is employed to calculate the eigenfrequency of the printer. Modes, as key parameters representing the free vibration characteristics of the system [5-6], correspond to different vibration modes at each order of frequency. Among them, the first-order mode has the lowest natural frequency, reflecting the most fundamental vibration mode of the system. As the mode order increases, the corresponding frequency values gradually increase, and the vibration modes become more complex. Considering that in practical engineering applications, the dynamic response of the system is mainly affected by the first few modes, this study focuses on analyzing the first six vibration modes of the high-precision ship-borne printer. In the aspect of external excitation response analysis, this study investigates the impact of various external excitations on the vibration of the high-precision ship-borne printer during navigation. The systematic analysis of the above two aspects can comprehensively evaluate the vibration characteristics of the printer in the practical application environment. Figure 1(b) illustrates the finite element mesh model of the high-precision ship-borne printer, which is discretized by using a combination of tetrahedral and hexahedral elements and contains a total of 6, 823, 579 nodes and 358, 126 elements. This refined mesh division ensures the accuracy of numerical calculation results, providing a reliable foundation for subsequent vibration characteristic analysis.

### 3 Results and Discussions

Eigenmode analysis is a classical research method of structural dynamics, which can effectively reveal key dynamic parameters such as natural frequencies and mode shapes of the structure. As the core component of the high-precision ship-borne printer, the high-precision printhead module consists of a series of high-precision components working in coordination. To simplify the vibration analysis model, the printhead module is equivalently modeled as a mass concentration point model in this study, with a focus on investigating the dynamic characteristics of its contact interface with the printer casing. As shown in Figure 1(b), the contact interface region is highlighted in red. This approximation method significantly improves the calculation efficiency while ensuring the analytical precision.

Firstly, the static characteristics of the high-precision ship-borne printer under gravity load are systematically studied. According to the design specifications, the total mass of the device is 120 kg. By applying a gravity load in the finite element model, the static deformation distribution of the system is obtained, as shown in Figure 2(b). The analysis results indicate that the maximum deformation of the system occurs in the structural region in contact with the high-precision printhead module, with a deformation magnitude of 0.37032 mm. In contrast, the minimum deformation is observed in the base plate region rigidly connected to the hull. This deformation distribution characteristic suggests that the structural stiffness of the printhead module's contact interface is relatively weak, which may have a significant impact on printing precision.

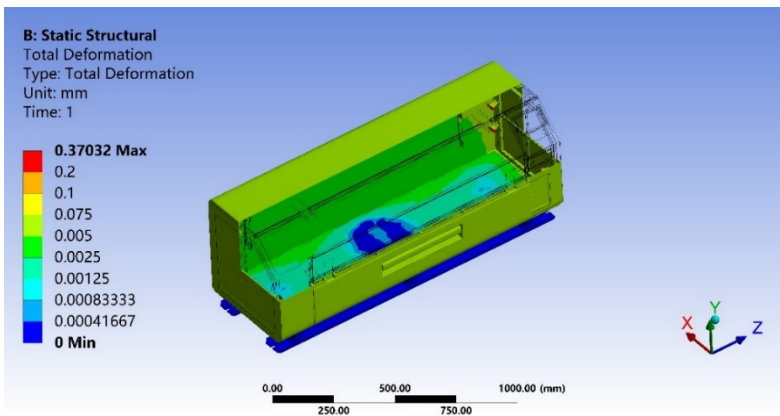


Fig. 2. Diagram of static deformation distribution of the high-precision ship-borne printer.

Based on the aforementioned analysis, the contact interface of the printhead module, as a key area for the structural integrity and dynamic performance of the high-precision ship-borne printer, requires special attention to analyze its stress distribution characteristics. To this end, a static equivalent stress analysis of the printer is conducted in this study, and the results are shown in Figure 3. The stress analysis results indicate a significant stress concentration at the contact interface of the printhead module, with maximum equivalent stress occurring at the edge of the contact interface, reaching 185.06

MPa. The analysis results provide an important basis for the subsequent structural optimization.

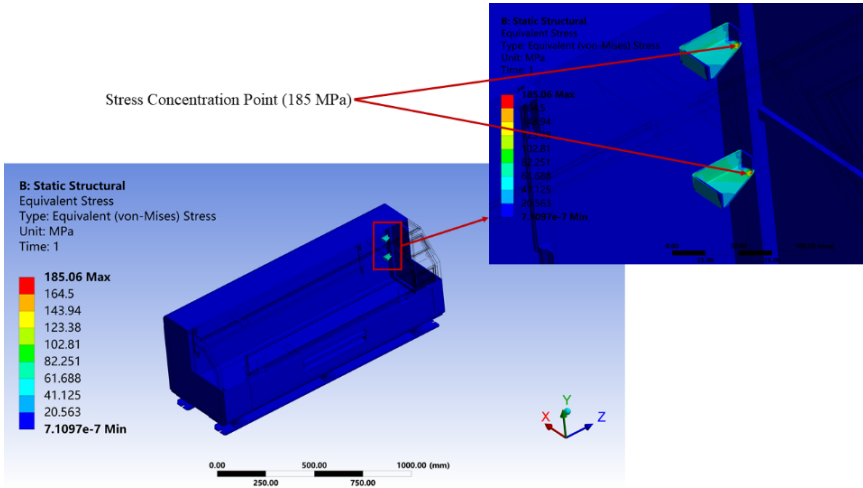
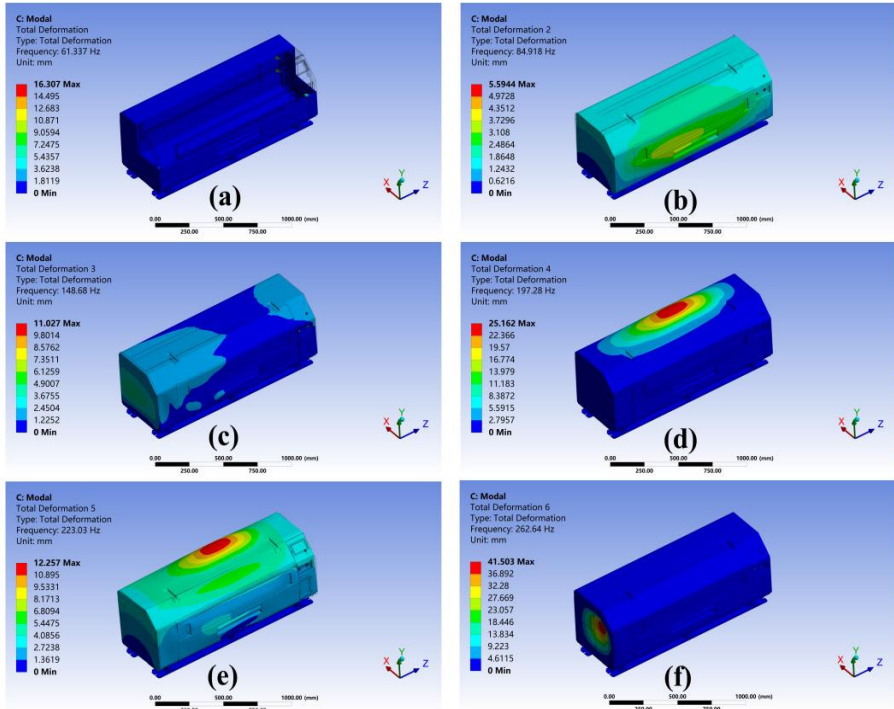


Fig. 3. Static equivalent stress distribution diagram of the high-precision ship-borne printer.

In this study, the characteristics of the first six modes of the high-precision ship-borne printer are obtained through modal analysis, with the results shown in Figure 4. The first six natural frequencies of the high-precision ship-borne printer are shown in Table 1. Figure 4(a) presents the analysis results of the first-order mode, which has a natural frequency of 61.337 Hz. This mode is mainly manifested by the local vibration in the supporting part of the printhead module, with a maximum deformation of 16.307 mm. Such vibration characteristics could directly affect the positioning accuracy of the printhead and print quality. Figure 4(b) depicts the characteristics of the second-order mode, with a natural frequency of 84.918 Hz. The vibration is mainly concentrated in the front panel area of the printer casing, manifested as a top bulging deformation, with a maximum deformation of 5.5944 mm, which may lead to contact problems between the casing and the internal components. The natural frequency of the third-order mode is 148.68 Hz, as shown in Figure 4(c), and its vibration is characterized by torsional deformation of the panels on both sides of the printer casing, with a maximum deformation of 11.027 mm. This torsional vibration could potentially induce structural fatigue issues. The natural frequency of the fourth-order mode is 197.28 Hz, as shown in Figure 4(d), and the vibration is mainly observed in the upper panel of the casing, which is manifested as a bulge in the central area, with a maximum deformation of 25.162 mm. Such large deformations may affect the overall stability of the printer. As shown in Figure 4(e), the fifth-order mode has a natural frequency of 223.03 Hz, and its vibration characteristics are similar to those of the fourth-order mode, but with an expanded vibration range covering the entire printer casing. This global vibration may exacerbate the printer's dynamic instability, with a maximum deformation of 12.257 mm. Finally, the natural frequency of the sixth-order mode is 262.64 Hz, as shown in Figure 4(f), and its vibration is mainly concentrated in the panel area on both sides, with a maximum

deformation of 41.503 mm, which is significantly higher than that of the fourth-order mode. Such large amplitude vibrations may lead to the risk of structural failure.

Through the systematic analysis of the first six modes, the dynamic characteristics of the high-precision ship-borne printer can be comprehensively understood, providing an important basis for subsequent structural optimization and vibration reduction design. In particular, the first three modes have the most significant impact on the printer's performance, requiring special attention and the implementation of corresponding vibration reduction measures.



**Fig. 4.** Modal shapes of the first six modes of the high-precision ship-borne printer.

**Table 1.** The first six natural frequencies of the high-precision ship-borne printer.

Order	Frequency/Hz	Vibration mode description
1	61.337	The local vibration in the supporting part of the printhead module
2	84.918	The vibration is mainly concentrated in the front panel area of the printer casing
3	148.68	The vibration is characterized by torsional deformation of the panels on both sides of the printer casing
4	197.28	The vibration is mainly observed in the upper panel of the casing
5	223.02	The vibration characteristics are similar to those of the fourth-order mode, but with an expanded vibration range covering the entire printer casing
6	262.64	The vibration is mainly concentrated in the panel area on both sides

In the study of the vibration characteristics of the high-precision ship-borne printer, in addition to the printer’s intrinsic modal vibration characteristics, the response vibration induced by external excitations is one of the key factors affecting its operational stability and precision. To comprehensively evaluate the vibration response of the printer in extreme environments, this study employs the power spectral density (PSD) data of sea surface vibration velocity under the condition of Category 12 typhoon as the excitation source [9-10] to simulate the vibration response characteristics of the printer under actual navigation conditions. The simulation analysis results are presented in Figure 5. The excitation response in the X-axis direction is shown in Figure 5(a), with a maximum displacement of 0.047725 mm and a confidence interval of 1  $\sigma$  (68.269%), indicating that the vibration response in this direction is relatively small, but it may still have a certain impact on the positioning accuracy of the printhead. The excitation response in the Y-axis direction is shown in Figure 5(b), with a maximum displacement of 0.14446 mm and a confidence interval of 1  $\sigma$  (68.269%). The Y-axis direction is the direction with the largest displacement among the three directions, which is closely related to the stiffness distribution characteristics of the printer’s structure in this direction, and may directly affect print quality and device stability. The excitation response in the Z-axis direction is shown in Figure 5(c), with a maximum displacement of 0.027317 mm, also within the 1  $\sigma$  confidence interval (68.269%). This represents the smallest displacement response, indicating that the printer has better vibration resistance in the vertical direction.

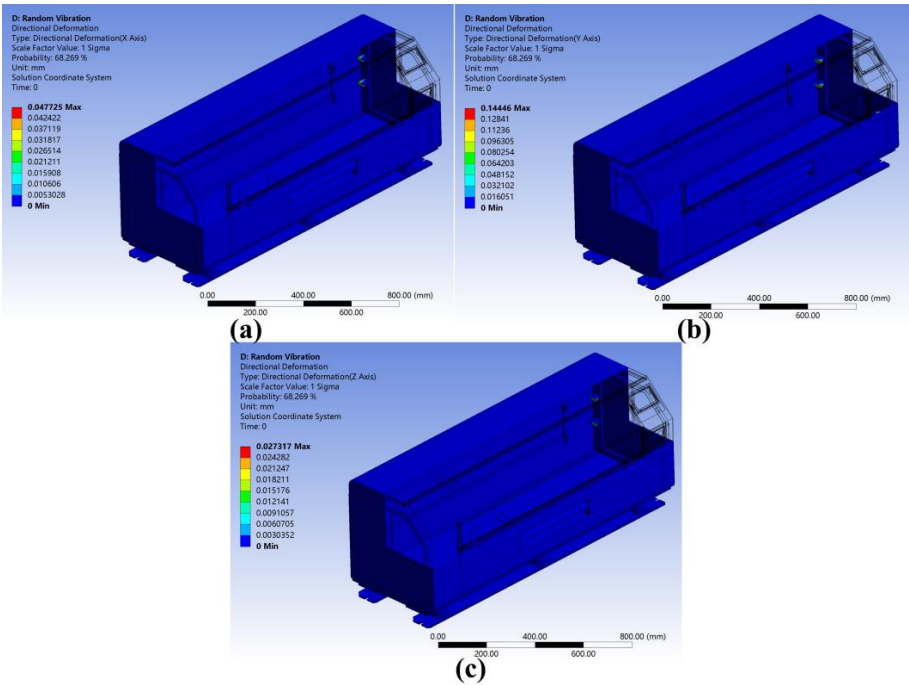
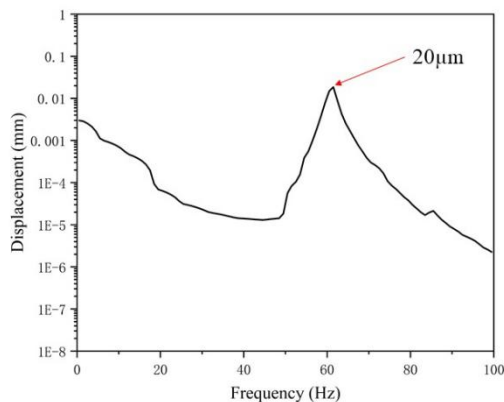


Fig. 5. Displacement distribution of the high-precision ship-borne printer under external excitations: (a) X-axis direction, (b) Y-axis direction, (c) Z-axis direction.

To further investigate the dynamic response characteristics in the Y-axis direction, this study quantitatively evaluates the displacement response along the Y-axis direction by employing the power spectral density analysis method. As shown in Figure 6, the displacement response power density spectrum in the Y-axis direction reveals the vibration characteristics of the system at different frequency bands. From the spectral analysis results, the following conclusions can be drawn: 1. Low-frequency response (below 50 Hz): The displacement response power density gradually decreases as frequency increases, indicating that the system exhibits better vibration resistance in the low-frequency range. This characteristic is attributed to the low-frequency modal suppression design of the printer, which effectively reduces the transmission efficiency of low-frequency vibrations. 2. Resonance peak characteristics (50–60 Hz): The power density spectrum shows a significant upward trend in the range of 50–60 Hz, reaching a peak near 60 Hz. Numerical integration calculations reveal that the maximum displacement response corresponding to this frequency band is  $20\ \mu\text{m}$ . The appearance of this resonance peak indicates a significant dynamic coupling effect near 60 Hz in the system, which may be related to the first-order modal characteristics of the printer. 3. High-frequency response (above 60 Hz): After exceeding 60 Hz, the displacement response power density exhibits a steady attenuation trend, benefiting from the good damping properties of the system in the high-frequency range, which effectively suppresses the accumulation of high-frequency vibration energy. It is noteworthy that, although a significant resonance response is observed near 60 Hz, the maximum displacement amplitude remains within  $20\ \mu\text{m}$ , which is far below the operational precision requirements of the printer.



**Fig. 6.** Displacement response power density spectrum in the Y-axis direction of the high-precision ship-borne printer.

## 4 Conclusion

Based on the above finite element analysis results, we can obtain the static structural characteristics and dynamic response spectrum of the high-precision ship-borne printer.

The natural frequency range of the first six modes of the printer varies from 61.337 Hz to 262.64 Hz. Among them, the first-order mode is mainly manifested by the local vibration of the printhead module's supporting part, with a maximum deformation of 16.307 mm, which significantly affects the printing precision. Under the condition of Category 12 typhoons, the maximum displacements of external excitation responses in the X, Y, and Z directions are 0.047725 mm, 0.14446 mm, and 0.027317 mm, respectively, among which the vibration response in the Y-axis direction is the most significant. The printer presents a significant resonance response near 60 Hz, but the maximum displacement remains within 20  $\mu\text{m}$ , indicating that the printer can maintain stable operation even in extreme environments. The above analysis results suggest that the stability optimization of the high-precision ship-borne printer should focus on optimizing the printer's static structural design, to further improve its operational stability. Through a systematic analysis of the dynamic characteristics, this study provides a theoretical basis for the structural design and performance optimization of high-precision ship-borne printers while also serving as technical references for the vibration control of high-precision devices in extreme environments.

## References

1. Wang C , Li Y , Lu J ,et al. Preparation and Characterization of a High-Stability, Low-Noise Ag/AgCl Sensor for Marine Electric Field Measurements[J].Journal of Ocean University of China, 2025, 24(2):332-342.
2. Moghaddas A A , Zeraatgar H .Numerical Investigation of the Effects of Aspect Ratio on the Hydrodynamic Performance of a Semi-Planing Catamaran[J].Polish Maritime Research, 2024, 31(3):25-33.
3. Petacco N , Gualeni P .The influence of ship stability in waves on naval vessel operational profiles[J].Journal of ocean engineering and marine energy, 2023, 9(4):681-695.
4. Risk analysis of bridge ship collision based on AIS data model and nonlinear finite element[J].Nonlinear Engineering, 2023, 12(1):102662-401.
5. Liu H , Zhai X , Hou Y ,et al.Thermal Analysis and Simulation of Protective Cover for Power Devices of BeiDou Antenna[C]. International Conference on Mechanical Design and Simulation.Springer, Singapore, 2025.
6. Zhu L , Wang X .Ship collision model tests in a water tank[J].Marine Structures, 2025, 103.
7. Mohan P .Numerical and experimental investigations on coupled motion response of ship and sloshing inside partially flooded compartments[J].Journal of Ocean Engineering and Marine Energy, 2025, 11(1):265-285.
8. Dong G , Yao C , Feng D . Study on Ship Motion in Waves with the Effect of Tank Sloshing[C]. The Proceedings of The Thirtieth (2020) International Ocean and Polar Engineering Conference.2020.
9. Hasselmann K . Measurements of wind-wave growth and swell decay during the Joint North Sea Wave Project (JONSWAP)[J].Dtsch.Hydrogr.Z, 1973, 8.
10. Kitaigorodskii S A . Applications of the theory of similarity to the analysis of wind-generated wave motion as a stochastic process[J].Izv.geophys.ser.acad.sci.ussr, 1962, 1.

**Open Access** This chapter is licensed under the terms of the Creative Commons Attribution-NonCommercial 4.0 International License (<http://creativecommons.org/licenses/by-nc/4.0/>), which permits any noncommercial use, sharing, adaptation, distribution and reproduction in any medium or format, as long as you give appropriate credit to the original author(s) and the source, provide a link to the Creative Commons license and indicate if changes were made.

The images or other third party material in this chapter are included in the chapter's Creative Commons license, unless indicated otherwise in a credit line to the material. If material is not included in the chapter's Creative Commons license and your intended use is not permitted by statutory regulation or exceeds the permitted use, you will need to obtain permission directly from the copyright holder.

